Analytical Methods

Accepted Manuscript

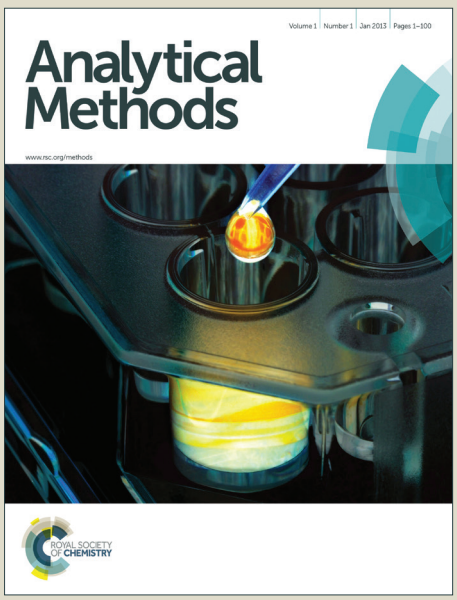

ROYAL SOCIETY OF CHEMISTRY

www.rsc.org/methods

Cite this: DOI: 10.1039/c0xx00000x

www.rsc.org/xxxxxx

FULL PAPER

A novel electrochemical sensor for non-ergoline dopamine agonist pramipexole based on electrochemically reduced graphene oxide nanoribbons

Prashanth S. Narayana [a], Nagappa L. Teradal [a], J. Seetharamappa [a]* and Ashis K. Satpati [b]

Received (in XXX, XXX) Xth XXXXXXXXX 20XX, Accepted Xth XXXXXXXXX 20XX
DOI: 10.1039/b000000x

A facile and feasible electrochemical sensing platform based on electrochemically reduced graphene oxide nanoribbons (ERGONRs) was designed for electrochemical investigations and determination of a non ergoline dopamine agonist, pramipexole dihydrochloride monohydrate (PPX) in pharmaceutical formulations and biological fluids. Newly synthesized graphene oxide nanoribbons were characterized by SEM, AFM, XRD and EDX. The solution of graphene oxide nanoribbons (GONR) was placed on glassy carbon electrode (GCE) and reduced electrochemically in phosphate buffer solution of pH 6 to obtain electrochemically reduced graphene oxide nanoribbons modified glassy carbon electrode (ERGONR-GCE). Significant electrooxidation of PPX was observed at ERGONR-GCE in phosphate buffer of pH 6.0 compared to that at bare GCE. Effect of accumulation time, pH and scan rate was studied and various electrochemical parameters were evaluated. The plot of pH versus E_p yielded a slope of 57.65 mV/pH in the pH range of 3.0-8.0 indicating the participation of equal number of electrons and protons in the electrode process. A differential pulse voltammetric method was developed for the determination of PPX in bulk, pharmaceutical formulations and urine samples. PPX showed linear relationship between the peak current and concentration in the range of 0.01 - 15 µM with LOD of 2.8 nM and LOQ of 9.4 nM. The fabricated electrode also showed good selectivity and excellent sensitivity. The proposed method is simple, rapid and inexpensive and hence, could be readily adopted for the analysis of PPX. The results were subjected to statistical analysis.

Introduction

The pursuit for increased sensitivity, selectivity and long-term stability of electrochemical sensors and biosensors, has generated a huge amount of research that directed to design active layers on electrodes. Recent advances in nanotechnology, electrochemical sensors and nanomaterials, have led to the development of simple and efficient tools to measure the concentration of analytes [1-4]. The use of graphene-based materials as electrode materials for electrochemical investigations is being investigated since, graphene is known for its exceptional mechanical, electronic, thermal and optical properties [5].

Graphene nanoribbons (GNRs) are thin elongated strips of sp^2 bonded carbon atoms that have captured worldwide interest. They are one-dimensional graphene-based materials like carbon nanotubes (CNTs), but exhibit different physico-chemical properties when compared to CNTs. Unlike CNTs in which their outer surface is mainly a basal graphitic plane, GNRs possess reactive edges. GNRs might even exhibit step-edges that could improve the adsorption and electrocatalysis of certain molecules on their surfaces [6]. Due to their various edge structures, GNRs present different electronic properties ranging from normal semiconductors to spin-polarized half metals that open up the possibility of using GNRs as electrochemical sensors. It is possible to synthesize graphene nanoribbons by the longitudinal unzipping of carbon nanotubes (CNTs) [7]. It is reported that the edge configuration (either zigzag or armchair) plays a primary role in the electronic properties of GNRs [8]. The edges are highly reactive. If GNRs are narrow, they might even behave as semiconducting or metallic one-dimensional wires depending on their edge termination [9]. Since, GNRs have large surface to volume ratio and special edge states, their properties can be modified by doping and adsorption processes. Due to their planar geometry and better water dispersibility, the fabrication and control of GNR nanostructures is simpler than that of CNTs. Extensive studies have been carried out on synthesis [20], electronic [8, 10-14], magnetic [15, 16], optical [17] and transport properties [18, 19] of GNRs.

Pramipexole (PPX), chemically known as (6S)-N6-propyl-4,5,6,7-tetrahydro-1,3- benzothiazole-2,6-diamine, is an orally active, non-ergoline, azepine derivative. It is a dopamine agonist used for the treatment of restless legs syndrome and Parkinson's disease. PPX is a novel aminobenzothiazole compound having highest affinity towards D3-subtype dopamine receptors [21-23].

PPX has an excellent oral bioavailability. Food does not influence the degree of absorption [24-26].

Literature survey revealed that only one voltammetric method [27] was reported for the assay of PPX. However, the reported voltammetric method uses bismuth for electrode modification. Bismuth is known to cause kidney damage and other health risks [28-31] and so its extensive use is not recommended. Moreover, the reported method is less sensitive (LOD = 12.79 ng mL-1) and needs longer time for drying the modified electrode at room temperature. In view of this, we have used graphene oxide nanoribbons for modification of the electrode and adapted an eco-friendly method for its reduction. The purpose of the present investigation is to develop an environmental-friendly, simple, sensitive and economically feasible sensor for the determination of PPX in tablets, human plasma and urine samples.

Experimental

Instrumentation

All electrochemical investigations were carried out on a CHI-1110a Electrochemical Analyzer (CH Instruments Ltd. Co., USA, v14.01). A three-electrode single compartment cell (10 mL) was connected to the Electrochemical Analyzer that consisted of a GCE or ERGONR-GCE (3 mm diameter) working electrode, a platinum wire auxiliary electrode and a saturated calomel (SCE) reference electrode. For good reproducible results, improved sensitivity and resolution of voltammetric peaks, the working electrode was abraded with 0.05 micron alumina slurry on a polishing cloth and thoroughly rinsed with milli-pore water. The cyclic and differential pulse voltammograms were recorded at 25±1 °C.

Powder XRD spectra were recorded on a Shimadzu XRD Maxima-7000 diffractometer with Cu Kα radiation. A Hitachi S-3400 (Japan) scanning electron microscope with an accelerating voltage of 15 kV was used to perform SEM studies. Composition analysis of samples was carried out on a Hitachi S-3400 SEM (Japan) attached with a Thermo Scientific EDX detector at an accelerating voltage of 15 kV and a magnification of 2 KX. Atomic force microscopic (AFM) images were taken on a Multi-Mode Nanosurf easyscan atomic force microscope (Nanosurf, Switzerland). The commercially available AFM cantilever tips (Tap190Al-G) with a force constant of 48 N/m and resonance vibration frequency of ~160 kHz were used.

Reagents

MWCNTs were purchased from Sigma-Aldrich (>99%). Pure PPX was obtained as a gift sample from Dr. Reddy's Laboratories at Hyderabad, India. Tablets of PPX were purchased from a local pharmacy. A stock solution of PPX (0.5 mM) was prepared in milli-pore water and stored in a refrigerator at 4 °C. Working solutions were prepared daily by diluting the stock solution as required with phosphate buffer (0.2 M) of required pH. In the present work, phosphate buffer (pH 3.0-10.6) was used. All solutions were prepared in milli-pore water and the chemicals used were of analytical reagent grade.

SEM/EDX

Films for SEM and Energy Dispersive X-ray Spectroscopic (EDX) analysis were prepared by placing sample suspension on carbon film coated on sample holder and drying at room temperature.

Synthesis of GONRs

GONRs were synthesized by unzipping of MWCNTs longitudinally using the procedure described elsewhere [7]. The GONR suspension was prepared by dispersing 10 mg of GONR in 10 mL water using ultrasonic agitation (1 h). This also led to the shortening of graphene oxide nanoribbons. The stable suspension was used to modify the GCE.

Electrode modification and electroreduction of GONR-GCE

Before modification, the GCE was cautiously abraded with 0.05 μm α-alumina slurry on a smooth polishing cloth, and then washed with milli-pore water. The cleaned GCE was coated by drop-casting 6 μL of the GONR suspension (1 mg mL^{-1}) and dried under infrared lamp to obtain a graphene oxide nanoribbon modified electrode (GONR-GCE). After modification, the electrode was rinsed with water to remove the loosely adsorbed GONRs. The GONR-GCE was then reduced electrochemically in phosphate buffer of pH 6.0 by applying five cyclic voltammetric sweeps in between 0.7 and -1.6 V to obtain electrochemically reduced GONR-GCE (ERGONR-GCE). The ERGONR-GCE was then transferred into 10 mL phosphate buffer of required pH containing a suitable amount of PPX and an accumulation time of 150 s was maintained. After 150 s, the voltammogram (either cyclic voltammogram or differential pulse voltammogram) was recorded. After every measurement, ERGONR-GCE was easily regenerated by cycling four voltammetric sweeps in the potential range of 0 to -1.6 V.

The electroactive surface areas of ERGONR-GCE and bare GCE were determined by CV using 1 mM $K_3[Fe(CN)_6]$ as a probe at different scan rates. For a reversible process, the Randles–Sevcik formula as shown below was used:

$$I_{pa} = 2.69 \times 10^5 \, n^{3/2} D_0^{1/2} \, C_0 \, \nu^{1/2} \quad (1)$$

where I_{pa} (A) is the anodic peak current, n is the electron transfer number, A (cm^2) is the surface area of the electrode, D_0 ($cm^2\ s^{-1}$) is the diffusion coefficient, C_0 (mol cm^{-3}) is the concentration of $K_3[Fe(CN)_6]$ and ν (V s^{-1}) is the scan rate. Using n = 1 and D_0 = 7.6×10^{-6} cm^2 s^{-1} for 1 mM $K_3[Fe(CN)_6]$ in 0.1 M KCl electrolyte, and the slope of plot of I_{pa} versus $\nu^{1/2}$, the electroactive surface area was calculated and found to be 0.058 and 0.148 cm^2 for bare GCE and ERGONR-GCE, respectively.

Analysis of tablets

Ten tablets (Zydus Cadila Healthcare Ltd., Ahmedabad, India) were ground to a homogeneous fine powder in a mortar. A fraction of the powder equivalent to 0.5 mM PPX was transferred to a 50 mL volumetric flask and completed to volume with milli-pore water. The contents of the flask were subjected to ultrasonication for 10 min to ensure that the active component was completely dissolved. Sample solutions of desired concentration were obtained by appropriate dilution of the clear supernatant liquid with the supporting electrolyte. Recovery experiments were carried out in order to examine the accuracy of the proposed method and to examine the interference from excipients generally used in the pharmaceutical formulation. The concentration of PPX in each sample solution was determined from the calibration plot or from the regression equation.

Determination of PPX in spiked human urine and plasma samples

Spiked urine samples were prepared by fortifying 9 mL urine with 1 mL PPX solution (5 mM) to obtain 0.5 mM PPX. Appropriate sample solutions were prepared by suitable dilution with phosphate buffer, without any pre-treatment and differential pulse voltammograms were recorded under optimized conditions.

Serum samples were taken from healthy individuals (after having obtained their written consent), were stored frozen until assay. For the determination of PPX in serum samples, 5 mL PPX solutions (1.25 mM) were added to 5 mL of untreated plasma. The mixture was shaken for 30 s. Perchloric acid (2.5 mL) was added to plasma samples to precipitate out plasma proteins. Then, the mixture was shaken for additional 30 s and then centrifuged at 5000 rpm for 5 min to separate the precipitated proteins. Appropriate amount of the solution was transferred in to the electrochemical cell containing phosphate buffer of pH 6.0 and differential pulse voltammogram was recorded. The voltammogram of blank (without PPX) did not show any signal that couldinterfere with the determination of PPX. The content of the drug in serum was determined from the calibration graph or regression equation.

Results and discussion

Characterization of GONRs

Graphene oxide nanoribbons (GONRs) were characterized by SEM, AFM, XRD and EDX analysis. Typical SEM images of MWCNT and GONR are shown in Figure 1A and 1B respectively. It is clear from the figure that the MWCNTs are not homogeneously dispersed while GONRs are evenly dispersed. This is due to the fact that the GONRs are soluble in water due the presence of hydroxyl groups. Elemental composition of GONRs was investigated by EDX and the results are shown in Table 1. The corresponding EDX spectrum of GONRs is shown in Figure 1B. It is evident that the GONRs consisted the elements viz., carbon and oxygen in major quantity besides other elements in trace quantities.

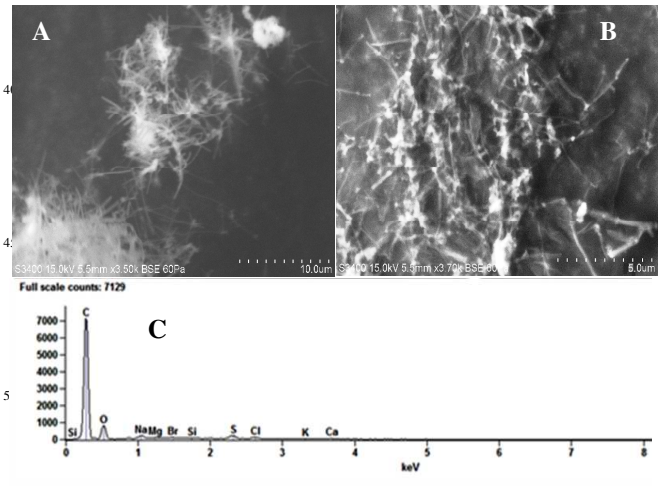

Fig. 1. Scanning electron micrographs of MWCNTs (A), GONR (B) and EDX of GONR(C).

Table 1. Chemical composition of GONR as obtained by Energy Dispersive X-Ray Spectroscopic analysis.

Element	Weight %
C	80.18
O	10.57
Na	1.80
Mg	0.20
Si	0.31
S	2.79
Cl	1.86
K	0.33
Ca	1.12
Br	0.84
Total	100

The XRD patterns of MWCNTs and GONRs are shown in Figure 2. MWCNTs exhibited a predominant peak at 26.25°. However, upon oxidative unzipping, it showed a diffraction peak at 8.11°. The complete disappearance of the peak at 26.25° and appearance of the new peak at 8.11° revealed that MWCNTs were completely oxidized to GONRs. Further, the interlayer spacing along the c-axis changed from 3.39 Å in pristine MWCNTs to 10.89 Å in GONRs. Such d-spacing was considerably larger than that of a single layer graphene. This could be attributed to the presence of oxygen-containing functional groups attached to edges of basal planes of GONR sheets and to the occurrence of atomic level roughness from structural defects (sp^3 bonding). So, individual graphene oxide sheets are anticipated to be thicker than individual pristine graphene sheets. At the same time, several ions could be inserted into the graphene layers thereby increasing the interlayer spacing [32-34].

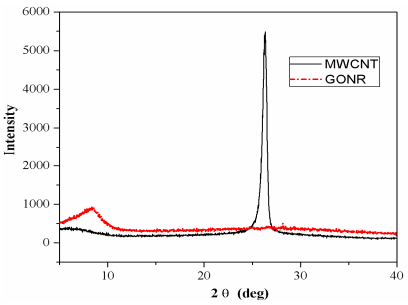

Fig. 2. XRD patterns of GONR (Red); MWCNTs (Black).

AFM studies were carried out to investigate the morphology, thickness of the films and the topography. It is clear from Figure 3A that the GONR sheets are wrinkled and well-dispersed. The GONR existed mainly as few layered structure and the average thickness of GONR sheets was found to be ~7 nm (Figure 3B). This is in agreement with the thickness of a few layered GONR. The 3-D topographic image is shown in Figure 3C. This indicated that the GONRs consisted of wrinkled structures that increased the surface area of the proposed electrode.

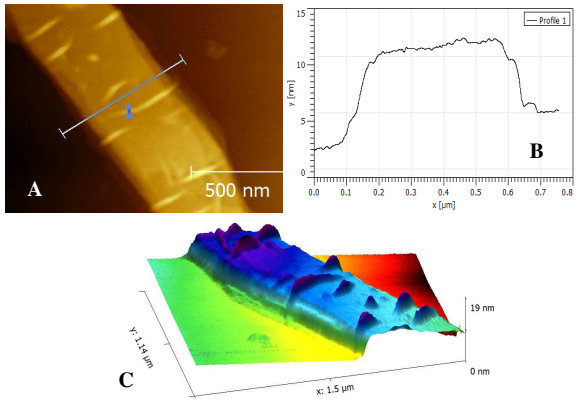

Fig. 3. (A) AFM image of GONR sheets; (B) Height profile of GONR sheets and (C) 3-D atomic force microscopic image of GONR film coated on a freshly cleaved mica sheet.

Electrochemical reduction of GONRs at GCE

The electrochemical reduction of GONR film at GCE was carried out in 0.2 M phosphate buffer of pH 6.0. This was achieved by cycling the potential between 0.7 and -1.6 V for 5 cycles (supplementary information, Fig. S1). A broad cathodic peak at a potential of ~ -1.1 V was observed in the first cycle which was attributed to the reduction of oxygen containing surface groups [35, 36]. Repetitive cycling of potential in electroreduction experiments indicated that the reductive peak currents of adsorbed GONRs on GCE surface decayed abruptly at the second and subsequent cycles. This indicated that most of the oxygen-containing groups on GONRs were reduced by electrochemical reduction.

Electrochemical behavior of PPX at ERGONR-GCE

Cyclic voltammograms of 5 µM PPX at different electrodes in phosphate buffer of pH 6.0 with a sweep rate of 100 mV s^{-1} are shown in Figure 4. Bare GCE showed no peak in the given potential range (curve a). However, it showed an irreversible oxidation peak at 0.85 V with a concentration of 25 µM PPX. A broad and poor oxidation peak at 0.79 V (curve c) was observed at electrochemically reduced graphene oxide modified GCE (ERGO-GCE). In contrast, an irreversible anodic peak was found at a peak potential of 0.83 V on ERGONR-GCE (curve b). The oxidation peak observed at ERGONR-GCE was sharper and well-defined compared to the one observed at ERGO-GCE. Further, the oxidation peak current was observed to be doubled at ERGONR-GCE (I_p = -23.4 µA) when compared to that at ERGO-GCE (I_p = -12.2 µA). This might be due to the presence of more number of electrochemical active sites in ERGONR-GCE than in ERGO-GCE. These electroactive sites were generated during the formation of ribbon like graphene structure. Hence, ERGONR-GCE was used as an electrochemical sensor for PPX.

Effect of pH

The influence of pH on electrooxidation of PPX at ERGONR-GCE was investigated in the pH range of 3.0 – 10.6 (Fig. 5). With increase in pH of the solution, the oxidation peak was observed to be shifted towards lower potentials indicating the involvement of proton(s) in the oxidation process. A slope value of 0.58 V pH^{-1} noticed in the plot of E_p versus pH (supplementary information, Fig. S2 A) revealed the participation of equal number of protons and electrons in the electrode process. Further, maximum peak current was noticed at pH 6.0 (supplementary information, Fig. S2 B). Therefore, buffer solution of pH 6.0 was used for subsequent work.

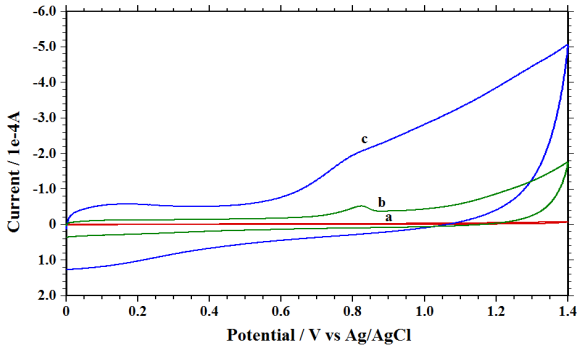

Fig. 4. Cyclic voltammograms of 5 µM PPX in phosphate buffer of pH 6.0 at (a) bare GCE, (b) ERGONR-GCE and (c) ERGO-GCE

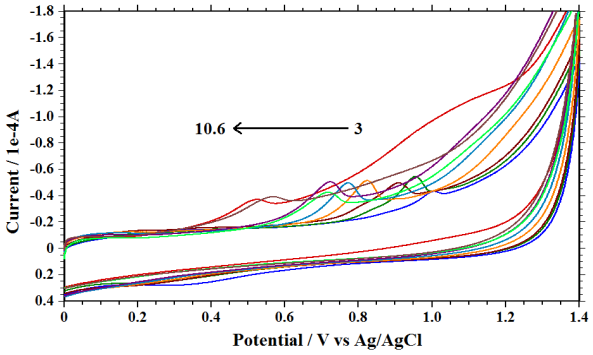

Fig. 5. Cyclic voltammograms of 5 µM PPX in phosphate buffer of different pH at a scan rate of 100 mV s^{-1}.

Effect of preconcentration time

Effect of preconcentration time on the oxidation peak current of PPX was examined. The oxidation peak current versus time plot indicated that the peak current of PPX increased upto 150 s and then leveled off. So, an accumulation time of 150 s was maintained.

Effect of accumulation potential

Accumulation potential plays a significant role in the electrochemical investigation of an analyte. So, we have investigated the effect of accumulation potential on electrooxidation of PPX at ERGONR-GCE. Maximum peak current was noticed at 0 V. Hence, accumulation was carried out at 0 V for further work.

Effect of potential sweep rate

Useful information with regard to electrochemical mechanism can be obtained from the relationship between the peak current

and sweep rate. Oxidation peak current exhibited linear dependence on the scan rate. The electro-oxidation peak current and peak potential increased with increase in the scan rate (Fig. 6) in the range of 0.005-0.4 V s^{-1} indicating the surface confined electro-oxidation process. Further, the plot of log ν versus log Ip yielded a slope value of 0.9937, confirming the above conclusion. The corresponding regression equation is given below:

$\log I_p = 0.9937 \log \nu - 0.6380 \qquad r^2 = 0.9965$

The electrochemical kinetic parameters *viz,* number of electrons transferred (n), electron transfer coefficient (α) and rate of the reaction were evaluated by subjecting the scan rate results to the Laviron equation [37,38]:

$$E_{pa} = E^{\circ\prime} + RT/\alpha nF\,[\ln (RTk_s)/(\alpha nF) - \ln \nu]$$

where $E^{\circ\prime}$ is the formal potential, n is the number of electrons transferred, α is the electron transfer coefficient and k_s is the standard rate constant of the electrode reaction. For irreversible oxidation reaction, the values of k_s and αn were deduced from the intercept and slope of the linear plot of E_{pa} vs. lnν, when the value of $E^{\circ\prime}$ was known. The value of $E^{\circ\prime}$ for PPX at ERGONR-GCE was obtained from the intercept of the plot E_{pa} vs. ν. Knowing the values of $E^{\circ\prime}$, the slope and intercept of the plot of E_{pa} vs. ν (Supplementary information, Fig. S3), the value of αn and k_s were calculated to be 1.12 and 1.41 s^{-1} respectively. Since, for a totally irreversible electron transfer reaction, α was assumed to be 0.5, the value of n was calculated to be 2. 24. This indicated that two electrons have taken part in the irreversible oxidation step.

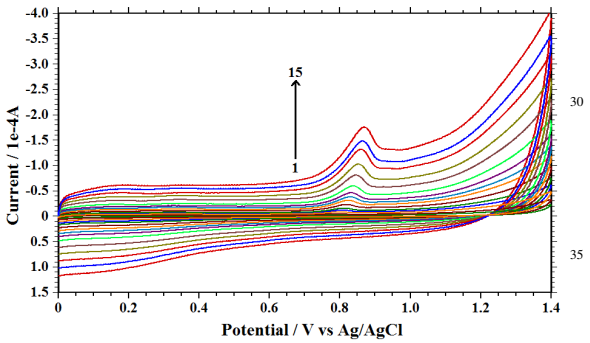

Fig. 6. Effect of scan rate on cyclic voltammograms of 5 µM PPX at (1) 5, (2) 10, (3) 20, (4) 30, (5) 40, (6) 60, (7) 80, (8) 100, (9) 120, (10) 150, (11) 200, (12) 250, (13) 300, (14) 350 and (15) 400 mV s^{-1}.

Construction of calibration plot

Differential pulse voltammetric technique is an effective and rapid electroanalytical technique having well-established advantages such as lower detection limits and good discrimination against background current. So, we have employed differential pulse voltammetric method to construct calibration graph. For this, voltammograms of increasing amounts of PPX were recorded (Fig.7). It was noticed that the peak current increased linearly with concentration of PPX. Linearity was noticed between the peak current and concentration of PPX in the range of 35 nM - 15 µM (inset of Fig 7). The corresponding regression equation is shown below:

I_p (µA) = 8.187 [PPX] (µM) + 0.530 (R^2=0.996).

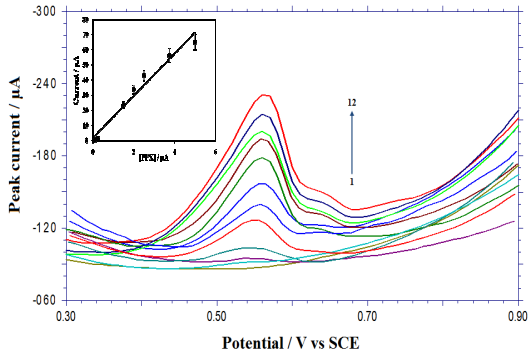

Fig. 7. Differential pulse voltammograms of PPX in phosphate buffer of pH 6.0. Inset: Calibration plot.

Table 2. Characteristics of calibration plot for PPX.

	DPV
Linearity (µM)	0.01 - 15.0
Slope (µAµM-1)	8.18
Intercept (µA)	0.053
Correlation coefficient	0.996
RSD (slope)* %	0.02
RSD (intercept)* %	1.44
LOD (nM)	2.8
LOQ (nM)	9.4
Inter-day assay RSD*, %	2.51
Intra-day assay RSD*, %	2.03

*Average of five determinations

Deviation from linearity was observed for solutions of higher concentration due to the adsorption of PPX or its oxidation product on the electrode surface. The analytical characteristics of the calibration plot are summarized in Table 2. The values of limits of detection (LOD) and limits of quantitation (LOQ) were calculated to be 2.8 nM and 9.4 nM, (n=6) respectively. Low values of LOD and LOQ confirmed the sensitivity of the proposed method. The lower RSD values for intra-day assay and inter-day assay (Table 2) indicated good reproducibility of the results.

Reproducibility and stability of the modified electrode

To find out the fabrication reproducibility of ERGONR-GCE, differential pulse voltammograms of 2.5 µM PPX were recorded on five independently prepared ERGONR-GCE. The RSD value for peak currents was calculated to be 3.12%, indicating the good fabrication reproducibility. The response of ERGONR-GCE for 2.5 µM PPX decreased by 4.27% of its initial response upon its storage at room temperature for three weeks. This revealed the long term stability of the modified electrode.

Interference studies

The selectivity of the proposed method was investigated by studying the effects of some generally occurring excipients on the electrooxidation current signal of PPX. The presence of an interferent that altered the average current signal of 2.5 µM PPX below ±5% was considered as non interference. It was observed that the talc, gum acacia and starch had no effect on the peak current up to 100-fold excess while glucose and sucrose did not exhibit any interference up to 125-fold-excess. Further, ascorbic

acid did not interfere with the determination of PPX up to 40-fold excess. These results demonstrated that the proposed DPV method for the assay of PPX was selective.

Analysis of tablets and statistical comparison of results with those of the reported method[27]

In order to evaluate the potential application of the developed DPV method, the tablets containing PPX (Parpex® tablets) were analyzed without any pretreatment and the results of analysis are given in Table 3. The validity of the proposed DPV method was further assessed by applying the standard addition method. The corresponding results of analysis were found to be satisfactory (Table 3). Further, the results were statistically compared with those of the reported voltammetric method [27]. Since, the calculated F-value (Table 3) did not exceed the tabulated value of 4.28 at 95% confidence level, we propose that there was no significant difference between the proposed and reported methods with respect to reproducibility. No significant difference in the accuracy between two methods was revealed by t-test value (Table 3) at 95% confidence level. These results demonstrated that the proposed DPV method utilizing the ERGONR-GCE was quite reliable and sensitive enough for the determination of PPX in tablets.

Recently reported method [27] employs a graphene/Bi_2O_3 modified electrode for the determination of PPX. The square wave voltammetric plot of PPX has shown a peak at 0.75 V. In the proposed method, differential pulse voltammetric peak was noticed at 0.55 V. The observed 200 mV decrease in the overvoltage revealed the easier electrochemical oxidation of PPX over ERGONR-GCE compared to that on the graphene/Bi_2O_3. Defect free wider graphene nano ribbons have showed excellent charge conducting properties. Generally, the chemical reduction of graphene oxide nanoribbon introduces defects in ribbon sheets resulting in the decreased electronic properties. In the present study, the electrochemical reduction process has produced defect free nanoribbons that have shown excellent charge transport property [39]. This was evident from the easy electrooxidation of PPX at ERGONR-GCE. The enhanced electron transfer property of PPX over ERGONR-GCE substrate has resulted in increased oxidation current and enhanced sensitivity.

Table 3. Results of analysis of PPX in commercial tablets.

Tablet	Parpex[a]	Found by the reported method[#]
Labeled claim (mg)	1.00	1.00
Amount found (mg)	0.99±0.016	0.98±0.008
Recovery[b] (%)	99.0	98.3
Bias[b] (%)	1.0	1.7
RSD[b] (%)	1.71	0.82
t- value at 95% confidence level	1.07	
F-value at 95% confidence level	4.0	
Tablet solution added (mg) to pure PPX solution	1.00	
Amount found (mg)	1.97	
Recovery[b] (%)	98.5	
Bias[b] (%)	1.5	
RSD[b] (%)	2.22	

[a] Marketed by Zydus Cadila Healthcare Ltd., Ahmedabad, India
[b] Average of 6 determinations.
[#] Reported voltammetric method using Bi_2O_3/GCE [27]

Determination of PPX in urine and plasma samples

The applicability of the proposed method was checked by determining PPX in spiked urine samples without any pre-treatment. The recovery of PPX from urine samples was examined by spiking the drug free urine with known amounts of PPX. The results of analysis are shown in Table 4. Higher recovery (more than 98.0%) and lower RSD values (less than 2.15%) revealed that the proposed method is accurate and precise.

Table 4. Results of analysis of PPX in spiked urine and serum samples at ERGONR-GCE.

PPX added (μM)	n	PPX found (μM)	Average recovery (%)	RSD[a] (%)
Urine samples				
1	5	0.98	98.0	1.89
8	5	8.10	101.25	2.07
15	5	14.91	99.4	2.15
Serum samples				
1	5	0.96	96.0	2.43
8	5	7.83	97.8	2.35
15	5	14.43	96.2	2.54

[a] Average of 5 determinations

The applicability of the proposed method was examined by analyzing PPX in plasma samples employing ERGONR-GCE. Serum samples were spiked with known amounts of PPX and analyzed by recording differential pulse voltammograms. The amount of PPX in the serum sample was determined by referring to the calibration plot. The results incorporated in Table 4 indicated good recovery of PPX.

Conclusions

In this work, a novel electrochemical sensing platform based on ERGONR film modified GCE was proposed for the assay of PPX. The proposed ERGONR-GCE showed fast electron transfer kinetics, larger electroactive surface area, higher sensitivity and stability. The exceptional properties of graphene nanoribbons combined with the 'green' nature of electroreduction may open up new avenues to use ERGONR as electrode modifier for the fabrication of electrochemical sensors for analytical applications.

Acknowledgements

We are grateful to the Board of Research in Nuclear Sciences, Mumbai, for financial assistance (No.2012/37C/8/BRNS/637 dated 28-05-2012). Thanks are also due to the authorities of the Karnatak University, Dharwad, for providing the necessary facilities.

Note and references

[a] *Department of Chemistry, Karnatak University, Dharwad-580 003, India.*
[b] *Analytical Chemistry Division, Bhabha Atomic Research Centre, Trombay, Mumbai 400 085, India*
[*] *Jaldappagari Seetharamappa (Corresponding author), Fax: +91-836-2747884; Tel: +91 836-221528; E-mail: jseetharam@yahoo.com*

[1] D. Hernandez-Santos, M. Diaz-Gonzales, M. B. Gonzales-Garcia and A. Costa-Garcia, *Anal Chem.*, 2004, **76**, 6887.
[2] J. Wang, *Anal. Chim. Acta*, 2003, **500**, 247.
[3] E. Katz, I. Willner and J. Wang, *Electroanalysis,* 2004, **16**, 19.
[4] X. Luo, A. Morrin, A. J. Killard and M. R. Smyth, Electroanalysis, 2006, **18,** 319.
[5] A. K. Geim and K. S. Novoselov, *Nat. Mater.,* 2007, **6**, () 183-191.
[6] R. Cruz-Silva, A. Morelos-Gómez, S. Vega-Díaz, F. Tristán-López, A. L. Elias, N. Perea-López, H. Muramatsu, T. Hayashi, K. Fujisawa, Y. A. Kim, M. Endo and M. Terrones, *ACS Nano,* 2013, **7**, 2192.
[7] D. V. Kosynkin, A. L. Higginbotham, A. Sinitskii, J. R. Lomeda, A. Dimiev, B. K. Price and J. M. Tour, *Nature*, 2009, **458**, 872.
[8] M. Fujita, K. Wakabayashi, K. Nakada and K. Kusakabe, J. *Phys. Soc. Jpn.,* 1996, **65**, 1920.
[9] M. Terrones, A. R. Botello-Méndez, J. Campos-Delgado, F. López-Urías, Y. I. Vega-Cantú, F. J. Rodríguez-Macías, A. L. Elías, E. Muñoz-Sandoval, A. G. Cano-Márquez, J. Charlier and H. Terrones, *Nano Today,* 2010, **5**, 351.
[10] K. Nakada, M. Fujita, G. Dresselhaus and M. S. Dresselhaus, *Phys. Rev. B.,* 1996, **54**, 17954.
[11] L. Brey and H. A. Fertig, *Phys. Rev. B,.* 2006, **73**, 195408.
[12] L. Brey and H. A. Fertig, *Phys. Rev. B.,* 2006, **73**, 235411.
[13] K. Wakabayashi, M. Sigrist and M. Fujita, *J. Phys. Soc. Jpn.,* 1998, 67, 2089.
[14] Y. Miyamoto, K. Nakada and M. Fujita, *Phys. Rev. B.,* 1999, **59**, 9858.
[15] K. Wakabayashi, M. Fujita, H. Ajiki and M. Sigrist, *Phys. Rev. B.,* 1999, **59**, 8271.
[16] C. P. Chang, C. L. Lu, F. L. Shyu, R. B. Chen, Y. C. Huang and M. F. Lin, *Physica E.*, 2005, **27**, 82.
[17] F. L. Shyu and M .F. Lin, *J. Phys. Soc. Jpn.,* 2000, **69**, 3529.
[18] K. Tada and K. Watanabe, *Phys. Rev. Lett.*, 2002, **88**, 127601.
[19] T. S. Li, Y. C. Huang, S. C. Chang and M. F. Lin, *Philosophical Magazine*, 2009, **89**, 697.
[20] M. Murakami, S. Iijima and S. Yoshimura, *J. Appl. Phys.,* 1986, **60**, 3856.
[21] J. Mierau, F. J. Schneider, H. A. Ensinger, C. L. Chio, M. E. Lajiness and R. M. Huff, *Eur. J. Pharmacol.,* 1995, **290**, 29.
[22] M. F. Finkel. *Arch. Neurol.,* 2000, **57**, 1519.
[23] M. H. Silber, M. Girish and R. Izurieta, *Sleep,* 2003, **26**, 819.
[24] M. D. Gottwaldov, J. L. Bainbridge, G. A. Dowling, M. J. Aminoff and B. K. Alldredge, *Ann. Pharmacother.,* 1997, **31**, 1205.
[25] N. Cotton, Process for preparing pramipexole dihydrochloride tablets, US patent. US2008/0254117 A1 2008.
[26] K. D. Tripathi, Jaypee Brothers Medical Publishers, New Delhi, 2003.
[27] R. Jain, R. Sharma, R. K. Yadav and R. Shrivastava, *J. Electrochem. Soc.,* 2013, **160**, H179.
[28] A. Erden, S. Karahan, K. Bulut, M. Basak, T. Aslan, A. Cetinkaya, H. Karagoz and D. Avci, *Int. J. Nephrol. Renovasc. Dis.*, 2013, **6**, 241.
[29] B. Bradley, M. Singleton and A. L. W. Po, *J. Clin. Pharm.,* 1989, **14**, 423.
[30] M. F. Gordon, R. I. Abrams, D. B. Rubin, W. B. Barr and D. D. Correa, *Mov. Disord.*, 1995, **10**, 220.
[31] A. Slikkerveer and F. A. de Wolff, *Med. Toxicol. Adverse Drug Exp.,* 1989, **4**, 303.
[32] C. Hontoria-Lucas, A. J. López-Peinado, J. de D. López-González, M. L. Rojas-Cervantes and R. M. Martín-Aranda, *Carbon,* 1995, **33**, 1585.
[33] H. He, T. Riedl, A. Lerf and J. Klinowski, *J. Phys. Chem.*, 1996, **100**, 19954.
[34] H. He, J. Klinowski, M. Forster and A. Lerf, *Chem. Phys. Lett.,* 1998, **287**, 53.
[35] T. Chen, Z. Sheng, K. Wang, F. Wang and X. Xia, *Chem. Asian J.,* 2011, **6**, 1210.
[36] H. L. Guo, X. F. Wang, Q. Y. Qian, F. B. Wang and X. H. Xia, *ACS Nano*, 2009, **3**, 2653.
[37] E. J. Laviron, *Electroanal.Chem.* 1979, **101**, 19.
[38] E. J. Laviron and L. J. Roullier, *Electroanal. Chem.* 1980. **115**, 65.
[39] K. A. Mkhoyan, A. W. Contryman, J. Silcox, D. A. Stewart, G. Eda, C. Mattevi, S. Miller and M. Chhowalla, *Nano Lett.*, 2009, **9**, 1058.